ADAPTIVE WAVEFORM SCHEDULING FOR TARGET TRACKING IN CLUTTER BY MULTISTATIC RADAR SYSTEM

Ngoc Hung Nguyen⋆*, Kutluyıl Doğançay*†⋆*, and Linda M. Davis*⋆

⋆Institute for Telecommunications Research, †School of Engineering
University of South Australia, Australia

ABSTRACT

An adaptive waveform scheduling algorithm is presented for target tracking by a multistatic radar system with two key components: (i) a distributed multistatic tracking algorithm for target tracking in cluttered environments, and (ii) the next transmitted waveform selected to minimize the tracking mean squared error. The scheduling algorithm is developed based on the minimization of the trace of the expected tracking error covariance matrix. A simulation example is presented to demonstrate the superiority of the proposed waveform scheduling algorithm over conventional fixed waveforms.

***Index Terms*—** adaptive waveform scheduling, multistatic radar, tracking, clutter, probabilistic data association

1. INTRODUCTION

In target tracking applications, the tracking performance can be significantly improved by dynamically changing the transmitted waveform to cope with changes in the target-radar geometry and the surrounding environment [1–5]. Extensive research has been conducted in adaptive waveform selection for monostatic radars. Early work in this area considered an one-dimensional target tracking problem [1, 2]. Further studies were conducted for target tracking in two-dimensional space for different scenarios of single/multiple targets, narrowband/wibeband environments, or clutter-free/cluttered environments in [3–5].

In contrast, adaptive waveform selection for target tracking by multistatic radars has received far less research attention. Multistatic radars with multiple transmitters and receivers are well-known for their performance advantage over monostatic radars [6]. Different to monostatic radars, the multistatic radar performance depends not only on transmitted waveform but also on radar geometry [7]. In a previous work [8], we have shown that the tracking performance of narrowband multistatic radars in clutter-free environments can be significantly improved by adaptive waveform selection.

In this paper, we extend our previous work to a more realistic scenario in which the probability of target detection is less than unity and clutter introduces unwanted false measurements at the receivers. A distributed multistatic tracking system incorporating local probabilistic data association - extended Kalman filters (PDA-EKF) is employed for tracking a single target in clutter. The adaptive waveform scheduling algorithm is developed to minimize the tracking mean squared error. This is achieved by selecting the next transmitted waveform parameters to minimize the trace of the expected tracking error covariance matrix. The expected tracking error covariance is computed using the measurement error covariance which is assumed to achieve the Cramér-Rao lower bound (CRLB) as commonly done in waveform selection literature. Note that the bistatic CRLB of the receiver-to-target range and bisector velocity has been derived in [9–11]. However, in the context of target tracking, the optimization criterion aims to minimize the error covariance of the tracking estimate (i.e. the estimates of target position and velocity) which can be readily computed from the bistatic CRLB of time delay and Doppler shift measurements. Therefore, in this paper we employ the bistatic CRLB of time delay and Doppler shift. The performance of the proposed waveform scheduling algorithm is compared with conventional fixed waveforms by Monte Carlo simulations.

2. MULTISTATIC RADAR SYSTEM

An active narrowband multistatic radar system with a dedicated transmitter and multiple receivers are considered, where each receiver incorporates a local PDA-EKF tracker and the transmitter incorporates a central processor which is responsible for combining local tracks and selecting the next transmitted waveform. At each receiver, measurements of time delay and Doppler shift are available and used by its local PDA-EKF filter to obtain a local track. The local tracks from all receivers are then sent to the transmitter for track combination and waveform selection. Communication links between the transmitter and receivers are assumed to be available with negligible time-synchronization errors.

3. BISTATIC NARROWBAND SIGNAL MODEL

In this paper, we restrict our study to narrowband environments. The standard model for monostatic narrowband sig-

978-1-4799-2893-4/14/$31.00 ©2014 IEEE

nals [12] was extended to the case of bistatic radar [13], where the transmitted and received signals are given by

$$s(t) = \sqrt{2}\mathrm{Re}[\sqrt{E_t}\tilde{s}(t)e^{j2\pi f_c t}] \tag{1a}$$

$$r(t) = \sqrt{2}\mathrm{Re}[(\sqrt{E_r}\tilde{s}(t-\tau)e^{j2\pi \upsilon t} + \tilde{n}(t))e^{j2\pi f_c t}] \tag{1b}$$

where $\tilde{s}(t)$ is the complex envelope of the transmitted signal, f_c is the carrier frequency, $\tilde{n}(t)$ is the baseband additive noise, τ is the total time delay, and υ is the Doppler shift. The total time delay and Doppler shift are given by [13–15]

$$\tau = R/c \quad \text{and} \quad \upsilon = f_c\dot{R}/c \tag{2}$$

where $R = R_T + R_R$ is the total range (R_T is the target-transmitter range and R_R is the target-receiver range), and c is the speed of light.

4. TARGET TRACKING IN CLUTTER

4.1. Target dynamic model

In this paper, we consider a two-dimensional tracking scenario, where $\mathbf{x}_k = [x_k, y_k, \dot{x}_k, \dot{y}_k]^T$ denotes the target state vector at time $k = 0, 1, \ldots$ with $[x_k, y_k]$ corresponding to the target position and $[\dot{x}_k, \dot{y}_k]$ corresponding to the target velocity. The target is assumed to move with a nearly constant velocity, which is modelled by

$$\mathbf{x}_{k+1} = \mathbf{F}\mathbf{x}_k + \mathbf{w}_k \tag{3}$$

where $\mathbf{w}_k$ is the process noise corresponding to the target maneuver, and $\mathbf{F}$ is the state transition matrix [16].

4.2. Measurement model

At time k, each receiver obtains the measurements of time delay and Doppler shift (denoted as τ_k^i and υ_k^i, respectively, at the i-th receiver). The measurement model at the i-th receiver is given by

$$\mathbf{z}_k^i = \begin{bmatrix}\tau_k^i \\ \upsilon_k^i\end{bmatrix} = \mathbf{h}^i(\mathbf{x}_k) + \mathbf{n}_k^i = \begin{bmatrix}\mathrm{h}_\tau^i(\mathbf{x}_k) \\ \mathrm{h}_\upsilon^i(\mathbf{x}_k)\end{bmatrix} + \begin{bmatrix}n_{\tau k}^i \\ n_{\upsilon k}^i\end{bmatrix} \tag{4}$$

where $\mathbf{n}_k^i$ is a white Gaussian noise which models the measurement error. Without loss of generality, we assume that the transmitter is located at the origin $[0,0]$ and the i-th receiver is located at $[x_{\mathrm{Rx}}^i, y_{\mathrm{Rx}}^i]$. Using (2), we can obtain the nonlinear transformations in (4) as follows:

$$\mathrm{h}_\tau^i(\mathbf{x}_k) = \frac{\|[x_k, y_k]\| + \|[x_k, y_k] - [x_{\mathrm{Rx}}^i, y_{\mathrm{Rx}}^i]\|}{c} \tag{5a}$$

$$\mathrm{h}_\upsilon^i(\mathbf{x}_k) = \frac{f_c}{c}\left(\frac{\dot{x}_k x_k + \dot{y}_k y_k}{\|[x_k, y_k]\|} + \frac{\dot{x}_k(x_k - x_{\mathrm{Rx}}^i) + \dot{y}_k(y_k - y_{\mathrm{Rx}}^i)}{\|[x_k, y_k] - [x_{\mathrm{Rx}}^i, y_{\mathrm{Rx}}^i]\|}\right) \tag{5b}$$

4.3. Measurement error

In this paper, we assume that the measurement errors $\mathbf{n}_k^i$ achieve their CRLB, hence the measurement error covariance $\mathbf{N}_k^i$ is assumed to be equal to the CRLB $\mathbf{C}_{(\tau,\upsilon)k}^i$ of the measurements of time delay τ_k^i and Doppler shift υ_k^i at the i-th receiver at time k. The CRLB for the measurements of time delay and Doppler shift was derived for monostatic radar in [12] and can be evaluated from the ambiguity function (AF) for a given waveform. The CRLB depends, among other things, on the transmitted waveform parameters [1, 12]. Since the bistatic ambiguity function with respect to time delay and Doppler shift remains the same as the corresponding monostatic ambiguity function [13], the CRLB for the measurements of time delay and Doppler shift derived in [12] can be used for the bistatic case. As a result, $\mathbf{C}_{(\tau,\upsilon)k}^i(\mathbf{\Omega})$, hence $\mathbf{N}_k^i(\mathbf{\Omega})$, is a function of the waveform parameters $\mathbf{\Omega}$. For a particular case of the Gaussian linear frequency modulated waveform class (Gaussian LFM) [4, 12], the CRLB $\mathbf{C}_{(\tau,\upsilon)k}^i(\mathbf{\Omega})$ at the i-th receiver is given by [8]

$$\mathbf{C}_{(\tau,\upsilon)k}^i = \frac{1}{\mathrm{SNR}_k^i}\begin{bmatrix}2\lambda^2 & -4b\lambda^2 \\ -4b\lambda^2 & \frac{1}{2\pi^2\lambda^2} + 8b^2\lambda^2\end{bmatrix} \tag{6}$$

where SNR_k^i is the signal-to-noise ratio at the i-th receiver at time k, λ is the Gaussian pulse length parameter, $b = \Delta_F/(2T_s)$ is the FM rate. Here Δ_F is the frequency sweep and $T_s \approx 7.4388\lambda$ [1] is the effective pulse length.

As noted in [13], the bistatic AF with respect to time delay and Doppler shift does not enable the direct evaluation of bistatic radar performance. Therefore, we do not use the CRLB of time delay and Doppler shift in the proposed waveform selection algorithm. However, it is still utilized to compute the tracking error covariance of the target state estimate (i.e. the target position $[x_k, y_k]$ and target velocity $[\dot{x}_k, \dot{y}_k]$) which is subsequently employed for evaluating the radar performance and selecting the appropriate transmitted waveform (see Section 5).

4.4. Clutter model

At time k, the measurements at each receiver consist of unwanted false measurements caused by clutter and the correct measurement (if it is detected). At the i-th receiver, the measurements are given by $\mathbf{Z}_k^i = [\mathbf{z}_{k(1)}^i, \mathbf{z}_{k(2)}^i, \ldots, \mathbf{z}_{k(m_k^i)}^i]$, where m_k^i is the number of measurements available at time k.

We assume that the false measurements are uniformly spatially distributed in the measurement space and independently across time; and the number of false measurements follow a Poisson distribution, where the probability mass function of the number of false measurements in the volume V is given by [17]

$$\mu(m) = e^{-\rho V}\frac{(\rho V)^m}{m!} \tag{7}$$

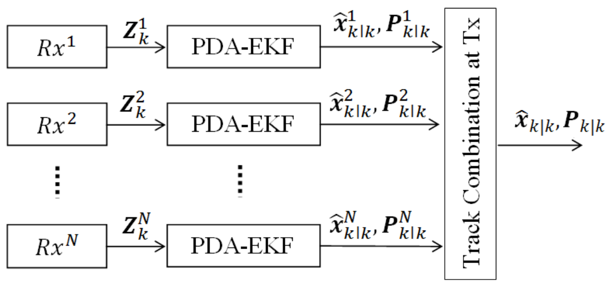

Fig. 1. Considered distributed tracking systems.

where ρ is the clutter density.

Furthermore, the probability of target detection of monostatic radar is $P_d = P_f^{1/(1+\text{SNR})}$ [3, 18], where P_f is the probability of false alarm and SNR is the signal-to-noise ratio at the receiver. Since the bistatic ambiguity function with respect to time delay and Doppler shift remains the same as the monostatic ambiguity function [13], the probability of target detection at the i-th receiver at time k is given by

$$P^i_{d_k} = P_f^{1/(1+\text{SNR}^i_k)}. \tag{8}$$

Note that SNR^i_k is dependent on the bistatic geometry and changes with time because of target motion.

4.5. Tracking algorithm

We consider a distributed tracking system as shown in Fig. 1, where at each receiver the measurements comprising the false measurements as well as the correct target-originated measurement are processed by a local probabilistic data association - extended Kalman filter (PDA-EKF) to obtain a local track. The local tracks from all receivers are sent to a central processor at the transmitter site for track combination.

Details of the PDA-EKF algorithm can be found in [16, 17]. The main idea of the PDA algorithm is that all validated measurements (those that fall inside the validation region) are considered as target-originated measurements with association probabilities and are used for updating the target state and tracking error covariance [16], while EKF can deal with the nonlinearity in the measurement model based on the first order Taylor series expansion [17].

In this paper, a simple approach of weighted linear combination of tracks [19] is employed ($\hat{\mathbf{x}}_{k|k} = \sum w_i \hat{\mathbf{x}}^i_{k|k}$ and $\mathbf{P}_{k|k} = \sum w_i \mathbf{P}^i_{k|k}$), where we choose the weighting coefficient corresponding to the i-th track as $w_i = \det(\mathbf{P}^i_{k|k})^{-1} / \sum(\det(\mathbf{P}^l_{k|k})^{-1})$ so that a track with a larger tracking error contributes less to the overall combined track. Note that, since our main focus is on adaptive waveform selection, this paper only employs a simple track-to-track fusion approach of weighted averaging where the correlation between tracks is not considered.

5. ADAPTIVE WAVEFORM SELECTION

We now present our adaptive waveform scheduling algorithm to minimize the overall tracking mean squared error (MSE) in both target position and velocity. This MSE is the trace of the tracking error covariance matrix [2]. Therefore, to optimize the tracking performance, we can select the next transmitted waveform at time $k+1$ (characterized by the waveform parameters $\mathbf{\Omega}_{k+1}$) to minimize $\text{Tr}(\mathbf{P}_{k+1|k+1})$. Thus,

$$\mathbf{\Omega}^*_{k+1} = \underset{\mathbf{\Omega}_{k+1} \in \text{Waveform-Library}}{\arg\min} \text{Tr}(\mathbf{P}_{k+1|k+1}(\mathbf{\Omega}_{k+1})) \tag{9}$$

Note that, similar to [1–5,8], in our problem $\mathbf{P}_{k+1|k+1}(\mathbf{\Omega}_{k+1})$ is also a function of the waveform parameter $\mathbf{\Omega}_{k+1}$.

However, due to the false measurements caused by clutter, $\mathbf{P}_{k+1|k+1}(\mathbf{\Omega}_{k+1})$ cannot be computed prior to time $k+1$ [2, 20, 21]. Therefore, instead of $\mathbf{P}_{k+1|k+1}(\mathbf{\Omega}_{k+1})$, we employ the expected value of the tracking error covariance $\overline{\mathbf{P}}_{k+1|k+1}(\mathbf{\Omega}_{k+1})$ as proposed in [21] which can be predicted prior to time $k+1$. For each receiver, $\overline{\mathbf{P}}^i_{k+1|k+1}(\mathbf{\Omega}_{k+1})$ can be computed as follows [21]

$$\overline{\mathbf{P}}^i_{k+1|k+1}(\mathbf{\Omega}_{k+1}) = \mathbf{P}^i_{k+1|k} - q^i_{2_{k+1}} \mathbf{O}^i_{k+1}(\mathbf{\Omega}_{k+1}) \tag{10}$$

where

$$\begin{aligned}
\mathbf{O}^i_{k+1}(\mathbf{\Omega}_{k+1}) &= \mathbf{K}^i_{k+1}(\mathbf{\Omega}_{k+1})\mathbf{S}^i_{k+1}(\mathbf{\Omega}_{k+1})\mathbf{K}^{iT}_{k+1}(\mathbf{\Omega}_{k+1}) \\
\mathbf{K}^i_{k+1}(\mathbf{\Omega}_{k+1}) &= \mathbf{P}^i_{k+1|k}\mathbf{H}^{iT}_{k+1}\mathbf{S}^i_{k+1}(\mathbf{\Omega}_{k+1})^{-1} \\
\mathbf{S}^i_{k+1}(\mathbf{\Omega}_{k+1}) &= \mathbf{H}^i_{k+1}\mathbf{P}^i_{k+1|k}\mathbf{H}^{iT}_{k+1} + \mathbf{N}^i_{k+1}(\mathbf{\Omega}_{k+1})
\end{aligned}$$

where $\mathbf{H}^i_{k+1}$ is the Jacobian maxtrix of $\mathbf{h}^i(\mathbf{x}_{k+1})$ [16] and $\mathbf{N}^i_{k+1}(\mathbf{\Omega}_{k+1})$ is the measurement error covariance which is assumed to be equal to the CRLB. The overall expected covariance is $\overline{\mathbf{P}}_{k+1|k+1}(\mathbf{\Omega}_{k+1}) = \sum w_i \overline{\mathbf{P}}^i_{k+1|k+1}(\mathbf{\Omega}_{k+1})$.

The scalar degradation factor $q^i_{2_{k+1}}$ in (10) is dependent on the clutter density ρ, the detection probability $P^i_{d_{k+1}}$, the validation gate volume V^i_{k+1}, and can be evaluated using Monte-Carlo integration [2, 20]. For a two-dimensional measurement and a 4-sigma validation gate, $q^i_{2_{k+1}}$ can be approximated by [20]

$$q^i_{2_{k+1}} \cong \frac{0.997\, P^i_{d_{k+1}}}{1 + 0.37(P^i_{d_{k+1}})^{-1.57}\rho V^i_{k+1}} \tag{12}$$

In this paper the optimal waveform $\mathbf{\Omega}^*_{k+1}$ in (9) is obtained by a finite grid search over available waveforms in a waveform library. For a large number of waveform candidates, the grid search is computational expensive, and hence a closed-form/approximate solution is required. However, this is out of scope of the current paper and will be investigated in our future work.

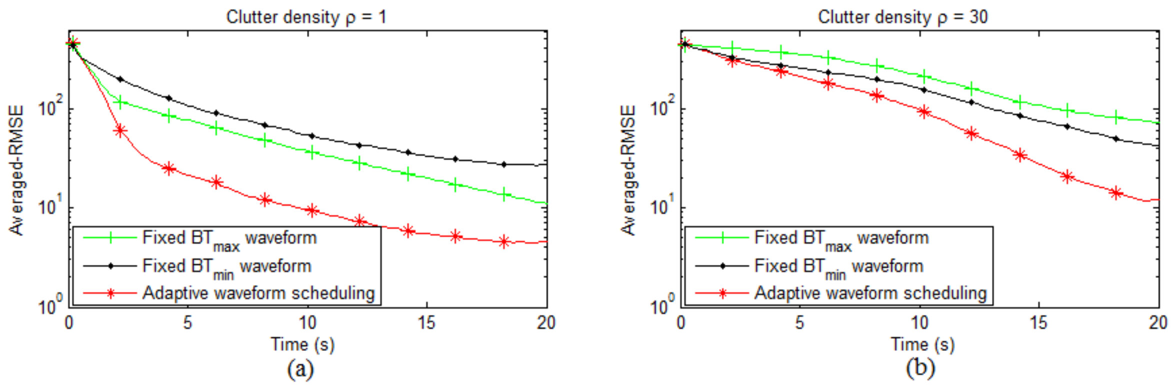

Fig. 2. Comparison of averaged-RMSEs of the proposed adaptive waveform scheduling and fixed waveforms with clutter densities: (a) $\rho = 1$ and (b) $\rho = 30$.

6. SIMULATION EXAMPLE

In this section, we simulate a specific tracking scenario with a transmitter located at the origin $[0, 0]$ m and four receivers located at $[20000, 0]$ m, $[10000, 15000]$ m, $[10000, -5000]$ m, and $[0, 10000]$ m. The initial position and velocity of the target are $[25000, 6000]$ m and $[-400, -200]$ m/s, respectively. The constant associated with the target maneuver [16] is $q = 10$. The carrier frequency is 12.5 GHz, and the pulse repetition interval is 200 ms. A Gaussian LFM waveform library is used with the parameters:$\lambda \in \{10, 28, 46, 64, 82, 100\}$ μs and $\Delta_F \in \{0.1, 0.28, 0.46, 0.82, 1\}$ MHz. The SNR at each receiver is modeled by $\mathrm{SNR}_k^i = R_0^4/(R_{Tk}^2 R_{Rk}^{i2})$, where $R_0 = 50000$ m. The probability of false alarm is $P_f = 0.01$ and a 4-sigma validation gate is used in the simulation. For each simulation run, a single track was initialized by a initial target state vector randomly generated from a normal distribution around the true target state vector as in [2, 3, 22] with the covariance of $P_{0|0} = \mathrm{diag}[(100\sqrt{10})^2, (100\sqrt{10})^2, 10^2, 10^2]$. A track is classified as lost if the correct measurement falls outside the validation gate for more than 4 consecutive time steps [2, 3, 22]. To evaluate the tracking performance, the averaged root mean squared error (averaged-RMSE) is computed from 500 converged tracks, where this average-RMSE includes errors in both target position and velocity.

Fig. 2 shows the comparison of the averaged-RMSE corresponding to the proposed adaptive waveform and the fixed waveforms with minimum and maximum time-bandwidth products ($\mathrm{BT}_{\min}$ and $\mathrm{BT}_{\max}$) for two clutter densities $\rho = 1$ and $\rho = 30$ false alarms per unit gate volume. We can see in Fig. 2a that the proposed adaptive waveform significantly reduces the tracking MSE compared to the fixed $\mathrm{BT}_{\min}$ and $\mathrm{BT}_{\max}$ waveforms for $\rho = 1$. The same observation is obtained for $\rho = 30$ in Fig. 2b, but the tracking performance of all waveforms are worse than the tracking performance of the corresponding waveforms in the case of $\rho = 1$ due to a higher clutter density ($\rho = 30$). Fig. 3 illustrates a pattern of the selected waveform parameters for a simulation run ($\rho = 30$).

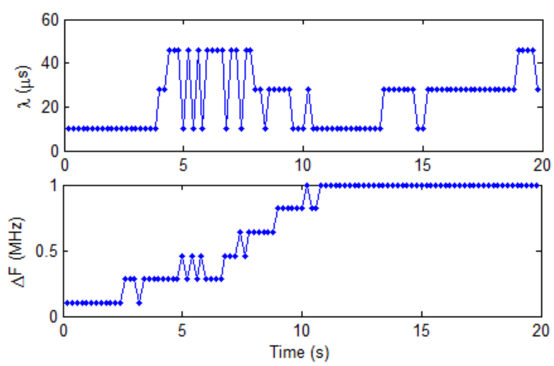

Fig. 3. Selected waveform parameters ($\rho = 30$).

We also observe that, in obtaining 500 converged tracks, the proposed algorithm causes 2 track losses compared to 2 track losses for the $\mathrm{BT}_{\min}$ waveform and 17 track losses for the $\mathrm{BT}_{\max}$ waveform for $\rho = 30$. For the lower clutter density $\rho = 1$, the numbers of track losses are 2, 0, and 9 for the proposed algorithm, the $\mathrm{BT}_{\min}$ waveform, and the $\mathrm{BT}_{\max}$ waveform, respectively. We can see that the proposed algorithm causes a much smaller number of track losses than the worse case of the fixed waveforms for the simulated tracking scenario.

7. CONCLUSION

In this paper we have investigated the problem of adaptive waveform selection for target tracking by multistatic radar in the presence of clutter, where a distributed multistatic tracking system incorporating PDA-EKF was employed for target tracking. The proposed adaptive waveform scheduling algorithm aims to minimize the tracking mean squared error via minimizing the trace of the expected tracking error covariance. The capability of the proposed algorithm to achieve a significant reduction in the tracking mean squared error was demonstrated with a simulation example.

8. REFERENCES

[1] D.J. Kershaw and R.J. Evans, "Optimal waveform selection for tracking systems," *Information Theory, IEEE Transactions on*, vol. 40, no. 5, pp. 1536–1550, 1994.

[2] D.J. Kershaw and R.J. Evans, "Waveform selective probabilistic data association," *Aerospace and Electronic Systems, IEEE Transactions on*, vol. 33, no. 4, pp. 1180–1188, 1997.

[3] S.P. Sira, A. Papandreou-Suppappola, and D. Morrell, "Dynamic configuration of time-varying waveforms for agile sensing and tracking in clutter," *Signal Processing, IEEE Transactions on*, vol. 55, no. 7, pp. 3207–3217, 2007.

[4] S.P. Sira, A. Papandreou-Suppappola, and D. Morrell, *Advances in Waveform-Agile Sensing for Tracking*, Synthesis Lectures on Algorithms and Software Engineering. Morgan and Claypool, 2009.

[5] S.P. Sira, A. Papandreou-Suppappola, and D. Morrell, "Waveform scheduling in wideband environments," in *IEEE International Conference on Acoustics, Speech and Signal Processing*, 2006.

[6] C.J. Baker, "An introduction to multistatic radar," *NATO Research and Technology Organisation Lecture Series RTO-EN-SET-133*, Apr. 2009.

[7] I. Bradaric, G.T. Capraro, and M.C. Wicks, "Waveform diversity and signal processing strategies in multistatic radar systems," in *Principles of waveform diversity and design*, M.C. Wicks, E.L. Mokole, S.D. Blunt, R.S. Schneible, and V.J. Amuso, Eds., chapter 16, pp. 286–304. SciTech Publishing, Raleigh, NC, 2010.

[8] N.H. Nguyen, K. Dogancay, and L.M. Davis, "Adaptive waveform selection for target tracking in multistatic radar systems," *Aerospace and Electronic Systems, IEEE Transactions on*, under review.

[9] M.S. Greco, P. Stinco, F. Gini, and A. Farina, "Cramér-Rao bounds and selection of bistatic channels for multistatic radar systems," *Aerospace and Electronic Systems, IEEE Transactions on*, vol. 47, no. 4, pp. 2934–2948, 2011.

[10] P. Stinco, M.S. Greco, F. Gini, and M. Rangaswamy, "Ambiguity function and Cramér-Rao bounds for universal mobile telecommunications system-based passive coherent location systems," *Radar, Sonar Navigation, IET*, vol. 6, no. 7, pp. 668–678, 2012.

[11] P. Stinco, M.S. Greco, F. Gini, and A. Farina, "Posterior Cramér-Rao lower bounds for passive bistatic radar tracking with uncertain target measurements," *Signal Processing*, vol. 93, no. 12, pp. 3528 – 3540, 2013.

[12] H.L. Van Trees, *Detection, Estimation, and Modulation Theory, Part III*, John Wiley and Sons, New York, 1971.

[13] T. Tsao, M. Slamani, P. Varshney, D. Weiner, H. Schwarzlander, and S. Borek, "Ambiguity function for a bistatic radar," *Aerospace and Electronic Systems, IEEE Transactions on*, vol. 33, no. 3, pp. 1041–1051, 1997.

[14] N.J. Willis, *Bistatic Radar*, SciTech Publishing, 2005.

[15] A. Farina, "Tracking function in bistatic and multistatic radar systems," *Communications, Radar and Signal Processing, IEE Proceedings F*, vol. 133, no. 7, pp. 630–637, 1986.

[16] Y. Bar-Shalom and W.D. Blair, *Multitarget-Multisensor Tracking: Applications and Advances, Volume III*, Artech House, Boston, 2000.

[17] Y. Bar-Shalom and X. Li, *Multitarget-Multisensor Tracking: Principles and Techniques*, YBS Publishing, Storrs, CT, 1995.

[18] C. Rago, P. Willett, and Y. Bar-Shalom, "Detection-tracking performance with combined waveforms," *Aerospace and Electronic Systems, IEEE Transactions on*, vol. 34, no. 2, pp. 612–624, 1998.

[19] A. Farina and F.A. Studer, *Radar data processing: vol. II - Advanced topics and applications*, Research Studies Press, UK, 1986.

[20] D.J. Kershaw and R.J. Evans, "A contribution to performance prediction for probabilistic data association tracking filters," *Aerospace and Electronic Systems, IEEE Transactions on*, vol. 32, no. 3, pp. 1143–1148, 1996.

[21] T. Fortmann, Y. Bar-Shalom, M. Scheffe, and S. Gelfand, "Detection thresholds for tracking in clutter–a connection between estimation and signal processing," *Automatic Control, IEEE Transactions on*, vol. 30, no. 3, pp. 221–229, 1985.

[22] Y. Bar-Shalom and T.E. Fortmann, *Tracking and Data Association*, Academic Press, San Diego, 1988.